Fuel xxx (xxxx) xxx

Contents lists available at ScienceDirect

Fuel

journal homepage: www.elsevier.com/locate/fuel

Full Length Article

Dehydrogenation of propane in the presence of CO_2 on GaO_x/SiO_2 catalyst: Influence of the texture characteristics of the support

Marina A. Tedeeva [a], Alexander L. Kustov [a,b,c], Petr V. Pribytkov [a,b], Gennady I. Kapustin [b], Alexander V. Leonov [a], Olga P. Tkachenko [b], Obid B. Tursunov [c,d,e,f], Nikolay D. Evdokimenko [b,c], Leonid M. Kustov [a,b,c,*]

[a] Department of Chemistry, M. V. Lomonosov Moscow State University, Moscow 119991, Russian Federation
[b] N. D. Zelinsky Institute of Organic Chemistry, Russian Academy of Sciences, Moscow 119991, Russian Federation
[c] National University of Science and Technology 'MISIS', Moscow 119049, Russian Federation
[d] Department of Power Supply and Renewable Energy Sources, Tashkent Institute of Irrigation and Agricultural Mechanization Engineers, Tashkent 100000, Uzbekistan
[e] Gulistan State University, Sir-Darya, Gulistan 120100, Uzbekistan
[f] School of Mechanical Engineering, Shanghai Jiao Tong University, Shanghai 200240, China

ARTICLE INFO

Keywords:
Propylene
Carbon dioxide
Gallium oxide
Propane oxidative dehydrogenation
Silica

ABSTRACT

GaO_x/SiO_2 catalytic systems with a gallium content of 3–50 wt% and deposited on SiO_2 with different texture characteristics were synthesized by incipient wetness impregnation. The effect of the support nature on the catalyst activity in the reaction of propane dehydrogenation in the presence of CO_2 was studied. The physicochemical properties of the supports and catalysts were characterized using low-temperature nitrogen adsorption, XRD, TPR-H_2, UV–Vis and diffuse reflectance FTIR spectroscopy, SEM, X-ray microanalysis, TEM, TG-DTA. It was found that a high dispersion of Ga_2O_3 particles on the support surface and a low acidity of the catalyst are required to achieve a high catalytic activity of Ga-containing catalytic systems. The best results were found for the catalyst supported on SiO_2 with a surface area of 747 m^2/g and a gallium content of 7 wt%, the propane conversion reached 33% with a propylene selectivity of 84%, and the stable operation time of the catalyst was more than 20 h.

1. Introduction

Propylene is an important raw material for the production of many chemical products. The main method for producing propylene is propane dehydrogenation, but this process is endothermic, requiring operation at relatively high temperatures and low pressures. Such process conditions favor undesirable thermal cracking reactions with production of lighter hydrocarbons and rapid catalyst deactivation due to coke formation.

An alternative to this process is the oxidative dehydrogenation of propane (ODP) in the presence of various oxidants such as O_2 [1,2], NO_2 [3–5], and CO_2 [6–9]. The advantage of the ODP process is that the reaction is carried out at lower temperatures with minimization of carbonization and catalyst deactivation [10–11].

Recently, a promising method for producing propylene is reported that is based on the oxidative dehydrogenation of propane in the presence of a mild oxidant - carbon dioxide ($C_3H_8 + CO_2 \rightarrow C_3H_6 + CO + H_2O$) [12]. Note that accumulation of CO_2 in the atmosphere leads to the climate changes on the planet. The presence of carbon dioxide in this reaction increases the equilibrium conversion by diluting propane, maintains the activity of the catalyst by inhibiting the formation of coke, and increases the conversion of propane by reducing the hydrogen concentration through the reverse water gas shift reaction ($CO_2 + H_2 = CO + H_2O$). In addition, CO_2 is involved in the coking process by the Boudouard reaction ($C + CO_2 \leftrightarrow 2CO$), removing some of the coke from the catalyst surface and thereby helping to maintain the stable activity of the catalyst.

The key problem in the use of CO_2 in the propane dehydrogenation process is the kinetic stability and inertness of the carbon dioxide molecule. Therefore, the development of highly efficient catalysts for the dehydrogenation of propane in the presence of CO_2 is an important task.

Ga-containing catalytic systems are promising catalysts for ODP-CO_2, which is explained by the unique structural characteristics of

* Corresponding author at: Department of Chemistry, M. V. Lomonosov Moscow State University, Moscow 119991, Russian Federation.
E-mail address: kyst@list.ru (L.M. Kustov).

https://doi.org/10.1016/j.fuel.2021.122698
Received 16 September 2021; Received in revised form 15 November 2021; Accepted 21 November 2021

coordinatively unsaturated surface centers [13–17] that are crucial for the activation of hydrocarbons in the CO_2 atmosphere. Earlier [18], we reported on the influence of the texture characteristics of the carrier on the activity of catalytic systems of the composition 2–10 wt% CrO_x/SiO_2. The dependence of the catalytic activity on the specific surface area and pore diameter of the carrier was established. Therefore, it is of interest to compare the catalytic activity of Ga-containing catalysts deposited on silica gel with different texture characteristics in order to obtain a highly selective and stable catalyst for the oxidative dehydrogenation of propane. To study the effect of the content of gallium oxide and the texture characteristics of the carrier on the performance of gallium catalysts, catalytic systems with a content of (3–50 wt%) gallium supported on SiO_2 with different texture characteristics have been studied in detail.

2. Experimental

2.1. Catalyst preparation

The catalysts were prepared by the method of incipient-wetness impregnation. Granular SiO_2 silica gels of Acros (SiO_2-A), KSKG (SiO_2-B), and Degussa (SiO_2-C) grades were used as carriers for the preparation of catalyst samples. The pre-crushed silica gel (fraction 0.25–0.5 mm) was dried in air at 100 °C for 6 h. The corresponding amount of Ga $(NO_3)_3{\cdot}H_2O$ was dissolved in distilled water and the carrier was impregnated. Then the samples were dried at a temperature of 100 °C for an hour.

The dried samples were calcined in air at a temperature of 650 °C for 4 h. Thus, Ga_2O_3 and the supported catalytic systems 3, 5, 7, 10, 30, 50 Ga/SiO_2-A, 3, 5, 7 Ga/SiO_2-B, and 3, 5, 7 Ga/SiO_2-C were obtained, the percentage is related to metallic gallium.

2.2. Catalyst characterization

The texture characteristics of the catalysts were determined based on the nitrogen adsorption isotherms measured at −296 °C using an ASAP 2020 Plus unit (Micromeritics Instrument Corporation, Norcross, GA/USA/). The specific surface area was calculated according to the BET method, and the pore size distribution was found from the desorption branch of the isotherm via Barrett–Joyner–Halenda (BJH) analysis. The volume of micropores was determined as the difference between the total pore volume and the comulative volume of mesopores at 2 nm in the BJH method.

The morphology, particle size, and elemental composition of the catalyst surface were studied by scanning electron microscopy (SEM) using a LEO EVO 50 XVP electron microscope (Carl Zeiss, Germany) equipped with an INCA Energy 350 energy dispersive spectrometer (Oxford Instruments, Great Britain). The device allows setting the energy of electrons in the range of 0.2–30 kV. The cathode is a heating element made of lanthanum hexaboride LaB_6.

Transmission electron microscopy was performed using a JEM 2100 instrument (JEOL, Japan) at an accelerating voltage of 200 kV. The catalyst powder was supported onto a copper mesh with an amorphous carbon coating, which was loaded into the TEM chamber.

Thermal analysis was performed with a combination of thermogravimetry, differential thermogravimetry, and differential thermal analysis (TG-DTG-DTA) with a Derivatograph-C unit (MOM). Each sample was placed into an alundum crucible and heated from 20 to 600 °C in air at the rate of 10 °C/min. α-Al_2O_3 was used as a standard; the weight of the samples was 100 mg.

X-ray diffraction (XRD) patterns of the samples were obtained with a DRON-2 diffractometer (CuK_α radiation). The samples were scanned in the 2θ range 20°–70° at a rate of 1 deg/min.

Temperature-programmed hydrogen reduction (TPR-H_2) was performed using a semi-automatic setup using a thermal conductivity detector calibrated by reduction of CuO (Aldrich-Chemie GmbH, 99+%, Steinheim, Germany) and a mixture of CuO + MgO (to be calibrated at low metal contents) pretreated in an Ar flow at 300 °C. The sample (100–150 mg) was also pretreated in argon at 300 °C for 1 h prior to the TPR experiment to remove water and other impurities. Then the sample was cooled to room temperature and the flow was switched to the reducing gas, and the sample was maintained at these conditions until the base line became stable (about 30 min). The sample was heated to 850 °C at a rate of 10 °C/min in a 5% H_2/Ar mixture flow (30 ml/min). Ar and H_2/Ar gases with a purity of 99.999% were purified additionally from oxygen using a trap containing a Mn/Al_2O_3 catalyst. Before TCD, the reduction products passed through a cold trap at −100 °C to remove H_2O. The presented TPR profiles were normalized per 1 g of the material.

Diffuse-reflectance UV–Vis spectra were obtained using a Shimadzu UV-3600 Plus spectrophotometer equipped with an ISR-603 integration sphere. The spectra were recorded at 200–800 nm at room temperature, and $BaSO_4$ was used as a standard and diluent. The weight of the catalysts was 0.1 g and that of $BaSO_4$ was 0.5 g. The UVProbe software was used to process the spectra.

Diffuse-reflectance FTIR (DRIFT) spectra were recorded at room temperature with a NICOLET "Protege" 460 spectrometer equipped with a diffuse-reflectance attachment in the range of 6000–400 cm^{-1} with a step of 4 cm^{-1}. For a satisfactory signal-to-noise ratio, 500 spectra were accumulated. CaF_2 powder was used as a standard. Before measuring the spectra, the samples were thermally treated in a vacuum at 400 °C for 2 h (heating rate of 5 °C/min) to remove physically adsorbed gases and water. Carbon monoxide was used as a test molecule for the electronic state of Ga. The adsorption was carried out at room temperature and an equilibrium pressure of CO 18 Torr. Deuterated acetonitrile was used as the test molecule for acid sites. Adsorption was carried out at room temperature and a saturated vapor pressure of CD_3CN (96 Torr).

The intensity of the bands in the spectra was expressed in Kubelka-Munk units [19,20]. The data were collected and processed using the OMNIC program. The spectra of adsorbed CO and CD_3CN were represented as the difference between those recorded after and before adsorption.

2.3. Catalytic tests

The dehydrogenation of propane to propylene in the presence of CO_2 was investigated at an atmospheric pressure in the temperature range 550–750 °C in a flow catalytic setup with a steel reactor with an inner diameter of 4 mm.

The gas mixture $C_3H_8 + CO_2$ was fed into the reactor in a volumetric ratio of 1:2, the total flow rate of the gas mixture was 30 ml/min. The catalyst loading was 1 g.

On-line analysis of the reaction products was carried out using a Chromatec-Crystal 5000 gas chromatograph equipped with a thermal-conductivity detectors, M ss316 3 m*2mm Hayesep Q and CaA molecular sieves 80/100 mesh columns. The temperature of the column was ramped according to the following program: 40 °C for 1.5 min, rising to 100 °C at a speed of 15 °C/min. The quantitative analysis was carried out by the absolute calibration method.

The propane conversion (C_p), propene yield (Y_p) and product selectivity (S_i) were calculated according to the following equations:

$$C_{C_3H_8}(\%) = \frac{(A_{C_3H_8})_{in} - (A_{C_3H_8})_{out}}{(A_{C_3H_8})_{in}} * 100;$$

$$S_{C_3H_6}(\%) = \frac{(A_{C_3H_6})}{(A_{C_3H_8})_{in} - (A_{C_3H_8})_{out}} * 100;$$

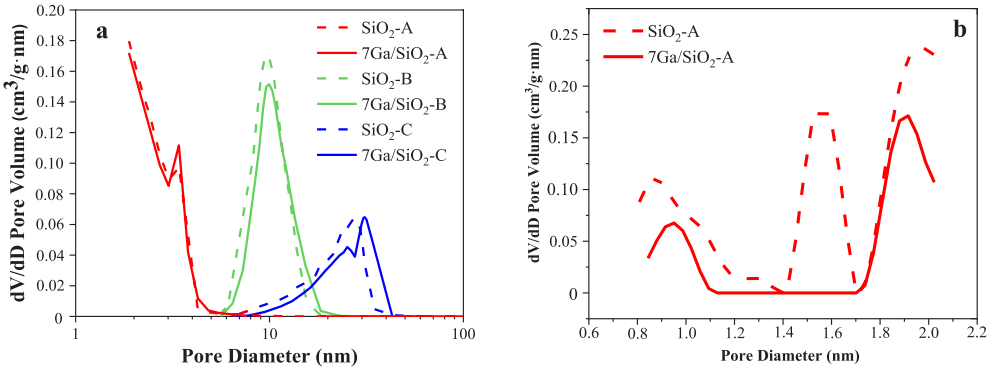

Fig. 1. a – Pore size distribution for SiO_2-A, SiO_2-B, SiO_2-C and 7 Ga/SiO_2-A, 7 Ga/SiO_2-B, 7 Ga/SiO_2-C catalysts (BJH-method), b – micropore size distribution for SiO_2-A and 7 Ga/SiO_2-A catalysts (DFT method. model: N_2-cylindrical pores – oxide surface).

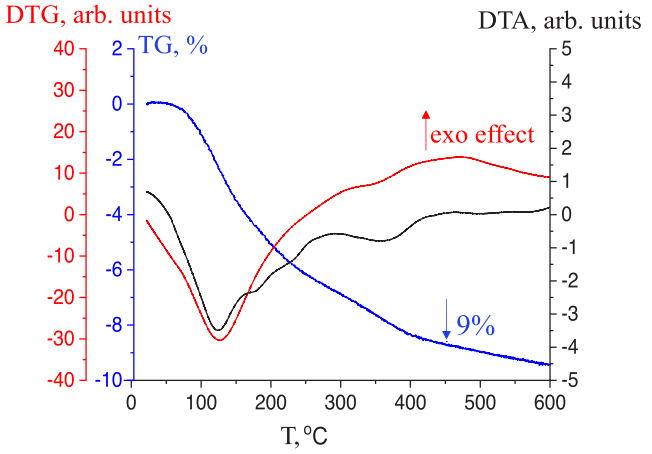

Fig. 2. Derivatogram of the 7 Ga/SiO_2-A catalyst dried in air at 100 °C for 1 h.

$$Y\ (\%) = \frac{C_{C_3H_8} * S_{C_3H_6}}{100};$$

where A is the component concentration.

3. Results and discussion

3.1. Physical and chemical properties of carriers and catalysts

The textural characteristics of the initial SiO_2-A, SiO_2-B, SiO_2-C and 7 Ga/SiO_2-A, 7 Ga/SiO_2-B, 7 Ga/SiO_2-C catalysts were investigated by low-temperature nitrogen adsorption. Isotherms are presented in Fig. S1 (Supplementary Information, SI).

Data on the textural characteristics of the starting samples and samples containing 7% Ga (Table S1, SI) show that micropores are present in SiO_2-A, the amount of which is 49.2% of the total pore volume in the sample. There are no micropores in SiO_2-B and SiO_2-C samples. We can see only mesopores with maxima of pore distribution curves at 10 and 12 nm for SiO_2-B and SiO_2-C samples, respectively (Fig. 1a). Micropores in SiO_2-A are responsible for the high value of the specific surface area of the sample. It should be noted that mesopores in SiO_2-A have a diameter of 2–5 nm and their specific surface area exceeds A_{BET} in SiO_2-B and SiO_2-C (Table S1). Although the volume of the mesopores in these samples is significantly greater than in SiO_2-A, these mesopores have a larger diameter than in SiO_2-A.

Introduction of 7% gallium leads to a decrease in pore volumes and the absolute value of the reducing V_{total} is maximum for 7 Ga/SiO_2-A. Analysis of micropores for SiO_2-A and 7 Ga/SiO_2-A by the DFT method (Fig. 1b) shows that micropores with d = 1.2–1.7 nm completely disappear. The volume of narrower and broader micropores is also reduced. The total volume of micropores is 66.2% of the starting sample. The volume of mesopores in the 7 Ga/SiO_2-A sample decreases by 27.1% compared with SiO_2-A. For the 7 Ga/SiO_2-B and 7 Ga/SiO_2-C samples, the mesopore volume decreased by 7% and 9%, respectively.

The thermal decomposition of gallium nitrate hydrate ($Ga(NO_3)_3$*xH_2O) on the support surface to gallium oxide was studied by the DTA-TG method. Fig. 2 shows a derivatogram of the 7 Ga/SiO_2-A sample obtained after drying at 100 °C for 1 h. The curves that characterize the changes in the mass of the sample (TG and DTG) and the thermal effects (DSC) observed with a linear rise in temperature to 600 °C are shown in Fig. 2.

There is a mass loss of about 5% in the temperature range from 25 to 150 °C, which is accompanied by heat absorption associated with the desorption of water from the surface and pores of the support. The decomposition of the crystal hydrate is observed in the range from 150 to 400 °C, followed by the decomposition of gallium nitrate. This process was accompanied by an endo-effect and a mass loss of about 4%.

It was concluded [21] that anhydrous gallium nitrate is not formed, since the reaction consists of related dehydration/decomposition processes occurring by a mechanism determined by the heating rate. TG measurements performed with isothermal stages (between 90 and 185 °C) show that $Ga(OH)_2NO_3$ is formed at the first stage of the reaction. Such a compound undergoes further decomposition to $Ga(OH)_3$ and $Ga(NO_3)O$, which are then decomposed to Ga(OH)O and finally to Ga_2O_3, respectively:

$Ga(OH)_2NO_{3(s)} \rightarrow (2/3)Ga(OH)_{3(s)} + (1/6)Ga_2O_{3(s)} + 2NO_{2(g)} + (1/2)O_{2(g)}$

$(2/3)Ga(OH)_{3(s)} \rightarrow (1/3)Ga_2O_{3(s)} + H_2O_{(g)}$

The SiO_2-A, SiO_2-B, SiO_2-C samples impregnated with a solution of gallium nitrate and calcined at a temperature of 650 °C were studied by scanning electron microscopy and transmission electron microscopy. According to the mapping presented in Fig. 3a, all the samples show a uniform distribution of gallium oxide particles, which is confirmed by the TEM data (Fig. 3b). According to the TEM data, all the samples demonstrate a uniform distribution of gallium oxide particles on the surface of the carrier with a particle size smaller than 3 nm, all samples exhibit ordered mesoporosity.

Elemental analysis of the sample surface was performed using energy-dispersion microanalysis (EDM). Table 1 and Fig. 3c show the spectra of characteristic X-ray emission and elemental analysis data for samples 7 Ga/SiO_2-A, 7 Ga/SiO_2-B, 7 Ga/SiO_2-C. Catalytic systems Ga/SiO_2-A and Ga/SiO_2-B show peaks corresponding to the lines of gallium, silicon, and oxygen, which indicates no impurities in the samples. An additional peak in the spectra of Ga/SiO_2-C catalysts is observed, which corresponds to calcium, with the actual content being 0.3%. It should be noted that, according to the energy dispersive microanalysis data, the nominal and actual gallium contents in the samples are close to each

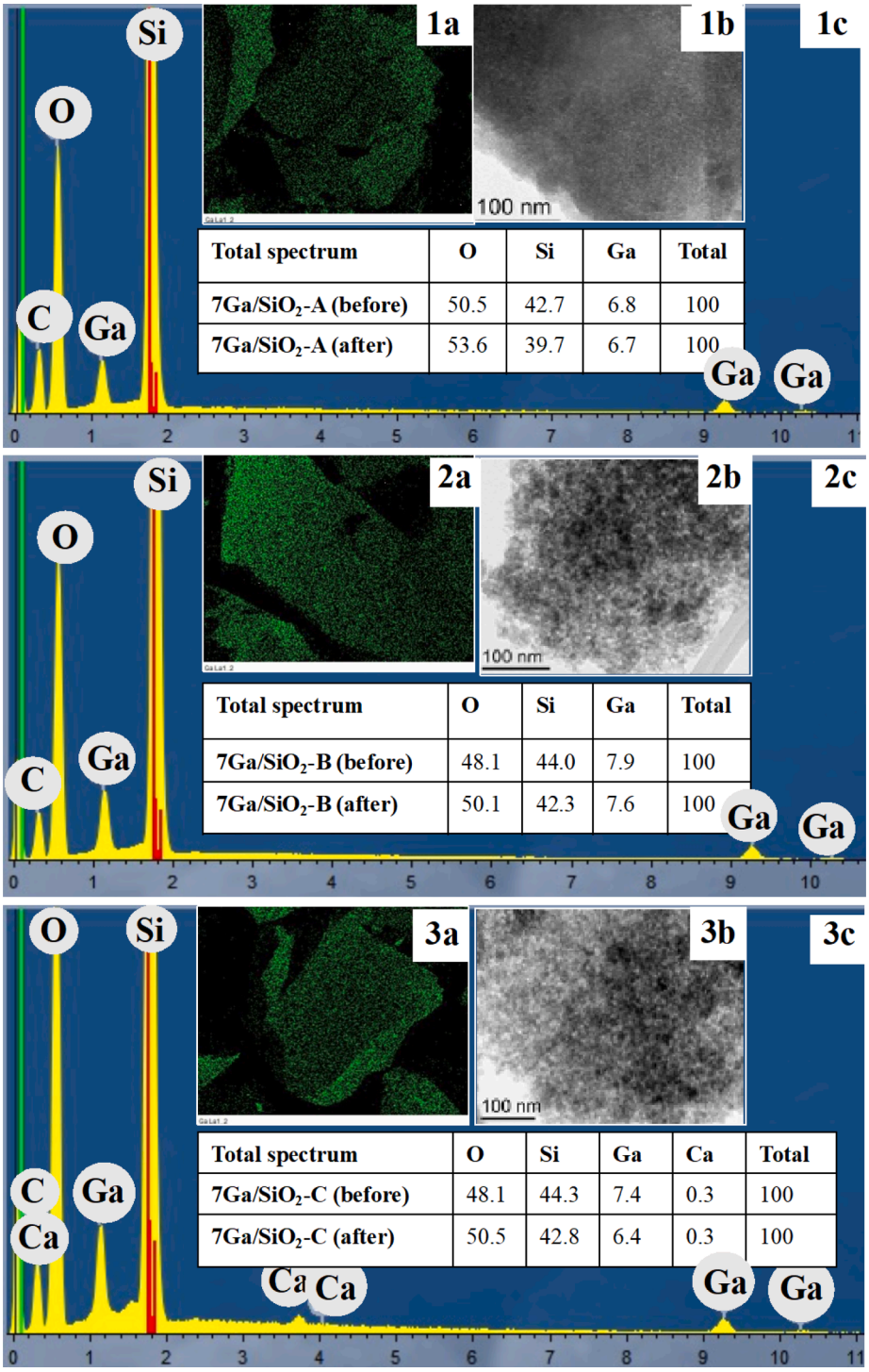

Fig. 3. SEM (a), TEM (b) and EDM (c) of 7 Ga/SiO_2-A (1), 7 Ga/SiO_2-B (2), 7 Ga/SiO_2-C (3) catalysts.

Table 1
Results of energy dispersive microanalysis (EDM) of the surface of catalytic systems.

Catalysts	O	Si	Ga	Ca	Total
3Ga/SiO_2-A	53.9	43.1	3.0	–	100
5Ga/SiO_2-A	52.7	42.5	4.8	–	100
3Ga/SiO_2-B	51.9	44.6	3.5	–	100
5Ga/SiO_2-B	51.5	45.8	2.6	–	100
3Ga/SiO_2-C	53.6	43.2	2.9	0.3	100
5Ga/SiO_2-C	53.1	43.6	3.0	0.3	100

other.

The crystal structure of the synthesized catalyst series Ga/SiO_2-A, Ga/SiO_2-B, and Ga/SiO_2-C containing 3, 5, and 7 wt% gallium was studied by X-ray phase analysis. However, no reflections on the diffractograms, except for the carrier reflexes, are observed in the case of the systems with a gallium content of 3, 5, and 7 wt%. This indicates that the gallium oxide on all carriers is well dispersed, and the particles have a size smaller than the coherent scattering region, i.e. 3–5 nm. This is also confirmed by the results of TEM (Fig. 3b). To confirm the crystal structure of gallium oxide on the carrier surface, samples of Ga_2O_3 and 30%Ga/SiO_2-A and 50%Ga/SiO_2-A were examined. The diffraction

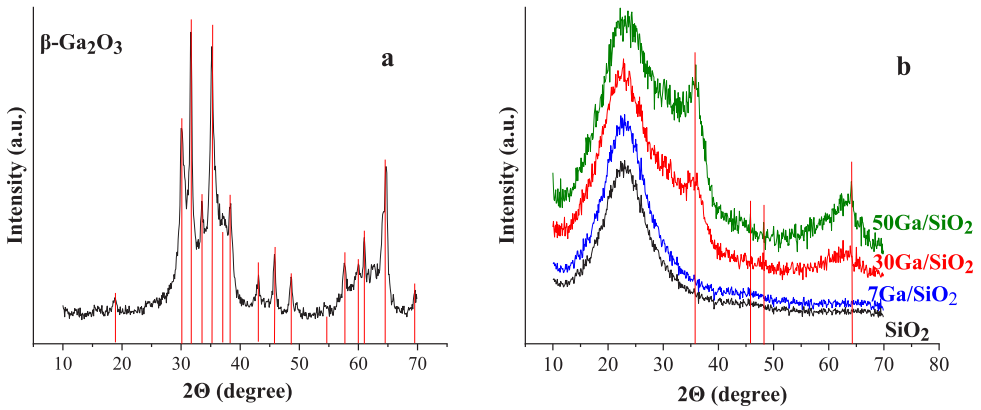

Fig. 4. XRD patterns: Ga_2O_3 (a), SiO_2-A, and 7 Ga/SiO_2-A, 30 Ga/SiO_2-A and 50 Ga/SiO_2-A (b) [JCPDS 43–1012].

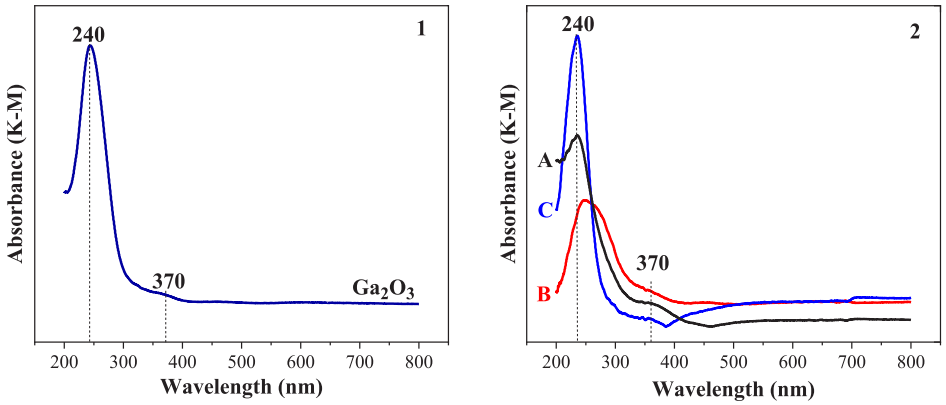

Fig. 5. UV–Vis diffuse reflectance spectra of Ga_2O_3 (1) and catalytic systems before catalysis (2): 7 Ga/SiO_2-A, 7 Ga/SiO_2-B, 7 Ga/SiO_2-C.

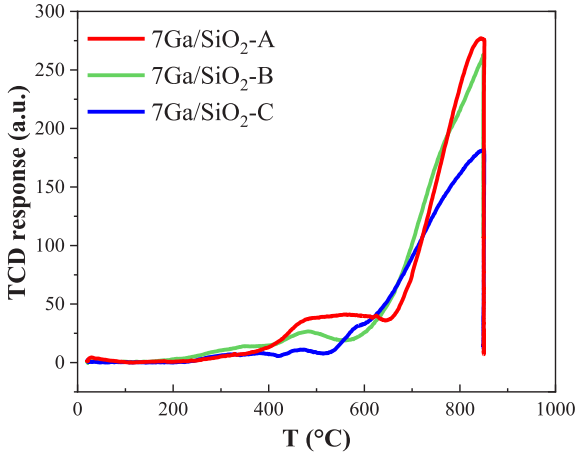

Fig. 6. TPR-H_2 patterns of 7 Ga/SiO_2-A, 7 Ga/SiO_2-B, and 7 Ga/SiO_2-C catalysts.

pattern is shown in Fig. 4a. Reflexes at 30.1°, 31.7°, 33.5°, 35.2°, 37.5°, 38.4°, 43.0°, 45.8°, 48.7°, 54.6°, 57.5°, 60.0°, 60.8°, and 64.7° correspond to the β-Ga_2O_3 phase [22]. The diffractograms of the 30%Ga/SiO_2-A and 50%Ga/SiO_2-A samples show reflexes at 35.2°, 45.8°, 48.7°, and 64.7° (Fig. 4b), which also correspond to β-Ga_2O_3.

Additional information about the structure of the catalysts was obtained using UV–Vis diffuse-reflectance spectra, the spectra of gallium oxide and the 7 Ga/SiO_2-A, 7 Ga/SiO_2-B, and 7 Ga/SiO_2-C catalytic systems before and after the catalytic tests are shown in Fig. 5. Gallium oxide (Fig. 5a) and catalytic systems (Fig. 5b) demonstrate an enhanced intensity of absorption with a wavelength significantly exceeding the optical absorption edge. According to the literature data [23], the bands at 250 and 370 nm correspond to β-Ga_2O_3, which is consistent with the results of X-ray phase analysis. A bathochromic effect is observed for all samples after catalysis, which may be associated with formation of coke on gallium oxide particles.

The reducibility of gallium oxide supported on silica carriers of different grades was studied using TPR- H_2 in the temperature range of 25–850 °C, the results are presented in Fig. 6 and Table S2.

The reduction peaks with maxima at about 300, 500, and 800 °C were found on the TPR-H_2 profiles for all three samples. The peak at 300 °C indicates that a small part of gallium oxide is reduced by hydrogen at low temperatures [22]. A peak at about 500 °C may indicate the reduction of extra-crystalline Ga_2O_3 (III) to Ga_2O (I) [24–26] according to the following reaction:

$$Ga_2O_3 + 3H_2 = Ga_2O + 3H_2O$$

To fully reduce all Ga^{3+} species in 1 g of the 7 Ga/SiO_2 sample, the amount of 1492 μmol H_2 is required, which is several times larger than the obtained values (Supplementary Information, Table S2). The amount of hydrogen consumed by catalytic systems for the reduction of easily reducible gallium ions decreases in the following order: SiO_2-A > SiO_2-B > SiO_2-C. So, for the SiO_2-A carrier, the amount of consumed hydrogen is 2–4 times larger than for the other carriers. It is possible that the low hydrogen consumption, especially for the 7 Ga/SiO_2-B and 7 Ga/SiO_2-C samples, is due to the formation of crystalline Ga_2O_3 on the support surface. When reducing Ga_2O_3 with hydrogen, the formation of metallic gallium is observed only as a result of high-temperature reduction of the sample under ultra-high vacuum conditions and is explained by the disproportionation of Ga^+ cations: 3 $Ga^+ \rightarrow 2\ Ga^0 + Ga^{3+}$ [27]. Indeed,

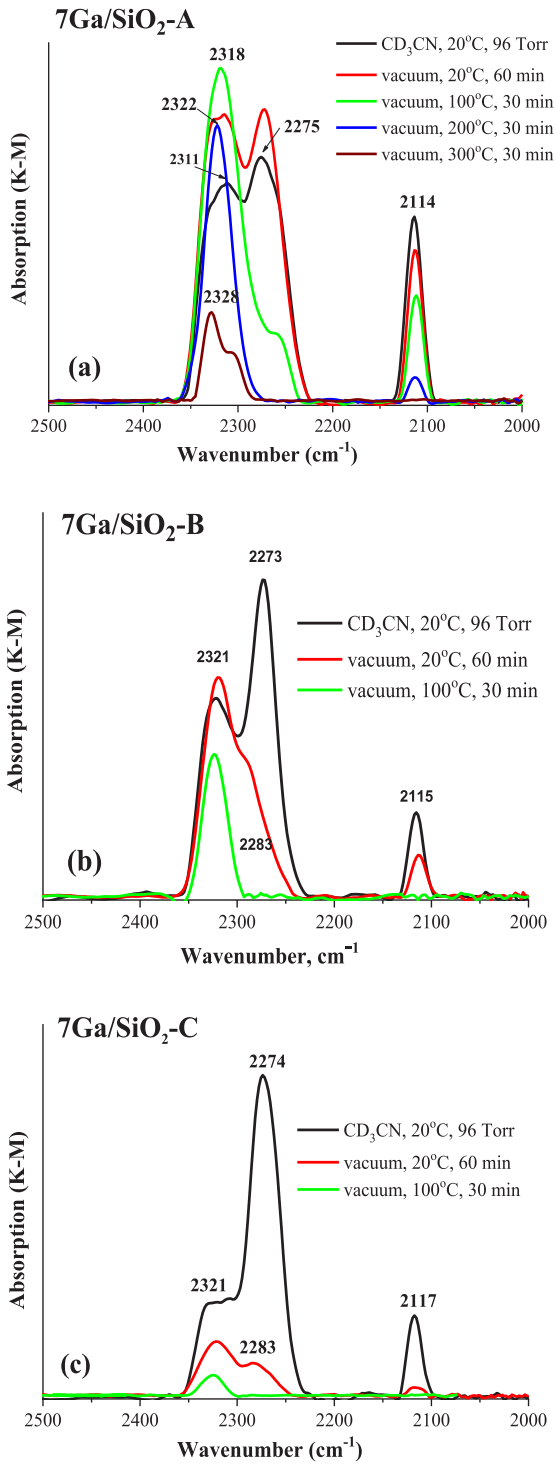

Fig. 7. DRIFT adsorption–desorption spectra of CD_3CN on: (a) 7 Ga/SiO_2-A; (b) 7 Ga/SiO_2-B; (c) 7 Ga/SiO_2-C.

the disproportionation reaction is typical for low-valent cations of elements of the third main group [27], but it should be noted that low-valent inorganic gallium compounds (Ga^+) are rather atypical. In the case of catalysts deposited on silicon dioxide, the presence of Ga^+ along with Ga^0 is possible, since, probably, in this case, the concentration of surface sites that contribute to the disproportionation of Ga^+ is low.

It has been shown in the literature that the activity of Ga-containing catalysts in propane dehydrogenation depends on both Lewis and Bronsted acid sites. The silicate support has a low concentration of medium and strong acid sites and a relatively high concentration of weak acid sites [15], the amount of which increases with the deposition of gallium oxide, which is an important factor in obtaining a stable and active gallium-containing catalyst. This fact was confirmed in the work [28] by adding potassium to the gallium oxide catalyst, which suppresses acidity, as a result, a decrease in the activity of the catalyst is observed. Information on acid-base sites for the obtained samples of catalysts and carriers was gained using FTIR spectroscopy. Three catalysts – 7 Ga/SiO_2-A, 7 Ga/SiO_2-B, and 7 Ga/SiO_2-C - were studied, and the supports were also investigated in order to determine the effect of the support on the properties of the supported catalysts.

In accordance with the DRIFT-CO spectra recorded for the supports and Ga-catalysts (Supplementary Information, Figs. S2-S4), a band at 2217–2220 cm^{-1} of different intensity appears in the spectra of all three catalysts in the presence of 18 Torr of CO. This band characterizes the stretching vibrations of the C≡O bond in the carbon monoxide molecule adsorbed on coordinatively unsaturated Ga^{3+} cations [19–20].

Deuterated acetonitrile was used as a test molecule for acid centers of catalysts and supports. Fig. 7 and Figs. S5-S7 (Supplementary Information) show the FTIR diffuse-reflectance spectra of OH groups recorded for three SiO_2 supports and three 7 Ga/SiO_2 catalysts after thermal vacuum treatment and adsorption of deuterated acetonitrile.

Three intense absorption bands (Supplementary Information, Figs. S5-S7) are observed in the spectra of supports and catalysts. According to the literature data [20,29–31], the band with a maximum at ~ 3700 cm^{-1} belongs to terminal isolated silanol groups (Si-OH). The absorption bands with a center at 3602 and 3557 cm^{-1}, respectively, are observed for SiO_2-A and SiO_2-B supports (Supplementary Information, Figs. S5b, S6b), which characterize the OH groups disturbed via the formation of hydrogen bonds. The absorption band at 3701 cm^{-1} for the catalyst 7 Ga/SiO_2-A (Supplementary Information, Fig. S5a) and the absorption bands at 3705 and 3677 cm^{-1} for the catalyst 7 Ga/SiO_2-B (Supplementary Information, Fig. S5b) are also assigned to the OH groups disturbed via hydrogen bonding. After adsorption of CD_3CN, the spectrum of OH groups broadens towards lower frequencies, and the peak intensity of the bands decreases. The difference between the spectra 2 and 1 gives the average value of the frequency shift of OH groups due to the formation of a complex with a hydrogen bond of acetonitrile molecules with Brønsted Acid Centers (BAC). Supports from different manufacturers are arranged in the following order according to the strength of BAC:

SiO_2-A > SiO_2-B > SiO_2-C.

It should be noted that the low acidity of SiO_2-C can be related to the calcium content.

According to the strength of BAC, the catalysts on these supports are arranged as follows:

7 Ga/SiO_2-A > 7 Ga/SiO_2-B > 7 Ga/SiO_2-C.

As can be seen, these series coincide, but it can be noted that when Ga is deposited on SiO_2-A and SiO_2-C, the BAC strength slightly increases, and when Ga is deposited on SiO_2-B, it does not change.

Fig. 7 and Fig. S8 (Supplementary Information) show the IR spectra in the range of OH group vibrations recorded during the adsorption–desorption of CD_3CN.

A band with a maximum at ~2275 cm^{-1} is observed in the spectra of all supports (Supplementary Information, Fig. S8) after adsorption of CD_3CN. This band corresponds to the coordination of acetonitrile molecules by BAC. The blue shift of the frequency of stretching vibrations of C≡N upon adsorption of CD_3CN on these centers is ~22 cm^{-1} as compared to the frequency in the gas phase (2253 cm^{-1}) [32]. This band completely disappears from the spectrum upon evacuation at 100 °C.

The spectra measured upon adsorption of CD_3CN on SiO_2-A, SiO_2-B, SiO_2-C supports contain bands with maxima at 2278 cm^{-1}, 2273 cm^{-1}, 2274 cm^{-1}, respectively (Supplementary Information, Fig. S8a-c), which correspond to coordination of acetonitrile molecules by acidic

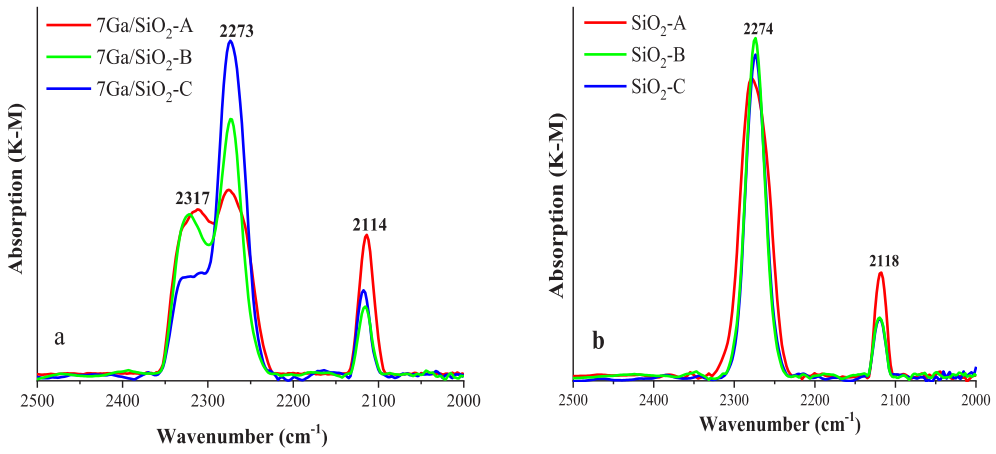

Fig. 8. (a) DRIFT-CD_3CN spectra of catalysts, (b) DRIFT-CD_3CN spectra of supports (Temperature – 20 °C, Pressure of acetonitrile – 96 Torr).

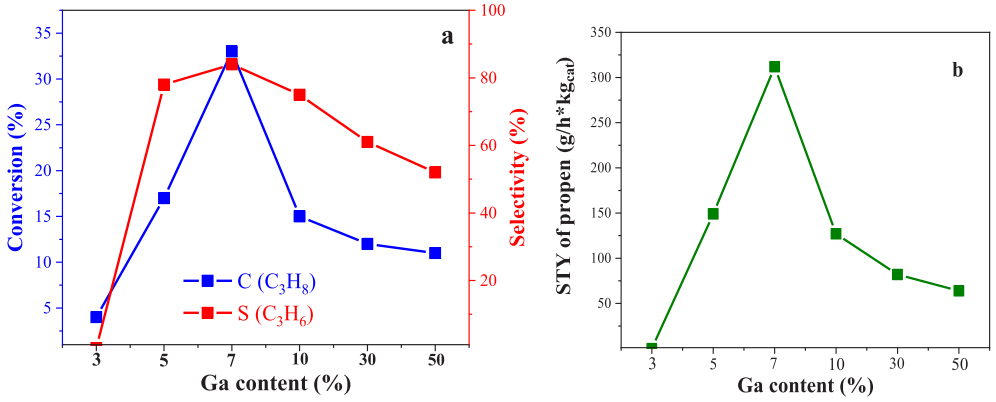

Fig. 9. Propane conversion, propylene selectivity (a) and space time yield of propene (b) for the 3, 5, 7, 10, 30, 50 Ga/SiO_2-A catalysts at a temperature of 650 °C.

centers - BAC. The blue shift of the C≡N stretching vibration frequency during adsorption of CD_3CN on these centers for SiO_2-A, SiO_2-B, SiO_2-C carriers is 25 cm^{-1}, 20 cm^{-1}, and 21 cm^{-1}, respectively, relative to the frequency in the gas phase (2253 cm^{-1}) [32]. This band completely disappears from the spectrum upon evacuation at 100 °C.

The spectra of the 7 Ga/SiO_2-A, 7 Ga/SiO_2-B, and 7 Ga/SiO_2-C catalysts manifest absorption bands with maxima at 2311 cm^{-1} (Fig. 7a), 2321 cm^{-1} (Fig. 7b), and 2321 cm^{-1} (Fig. 7c), respectively, which correspond to the coordination of acetonitrile molecules by Lewis acid centers - LAC (Ga^{3+} cations) [29–31]. The blue shift of the C≡N stretching vibration frequency during adsorption of CD_3CN on these sites is 58 cm^{-1} for the 7 Ga/SiO_2-A catalyst and 68 cm^{-1} for the 7 Ga/SiO_2-B and 7 Ga/SiO_2-C catalysts relative to the frequency in the gas phase (2253 cm^{-1}) [32]. In addition, the spectra of the 7 Ga/SiO_2-A, 7 Ga/SiO_2-B, and 7 Ga/SiO_2-C catalysts contain the band of adsorbed acetonitrile at 2275 cm^{-1}, 2273 cm^{-1}, 2274 cm^{-1}, respectively, which corresponds to the coordination of acetonitrile molecules with Brønsted acid centers. The blue shift of the C≡N stretching vibration frequency during the adsorption of CD_3CN on these sites for the 7 Ga/SiO_2-A, 7 Ga/SiO_2-B, and 7 Ga/SiO_2-C catalysts is 22 cm^{-1}, 20 cm^{-1}, and 21 cm^{-1}, respectively. The bands of CD_3CN adsorbed on BAC are the first to disappear; on the contrary, the bands of CD_3CN coordinated on the LAC are retained in the spectrum up to the evacuation temperature of 100 °C.

Fig. 8 (a) and (b) compare the spectra of adsorbed CD_3CN on all

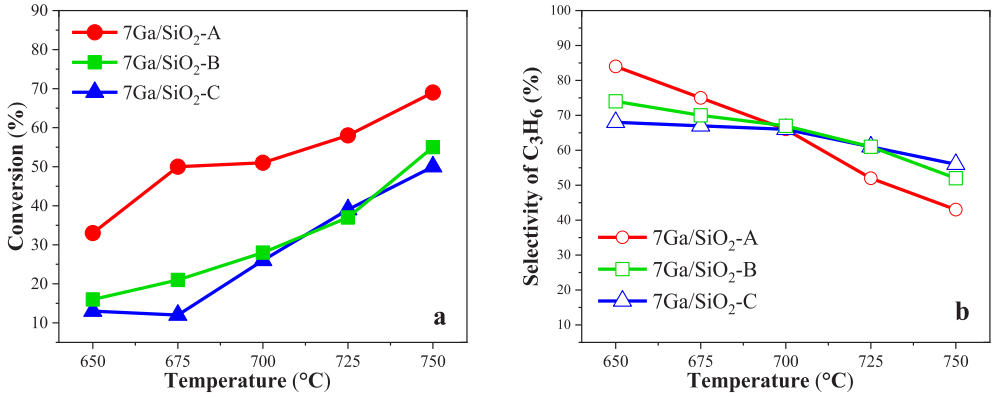

Fig. 10. Dependence of (a) propane conversion and (b) propylene selectivity on the reaction temperature for the 7 Ga/SiO_2 catalysts.

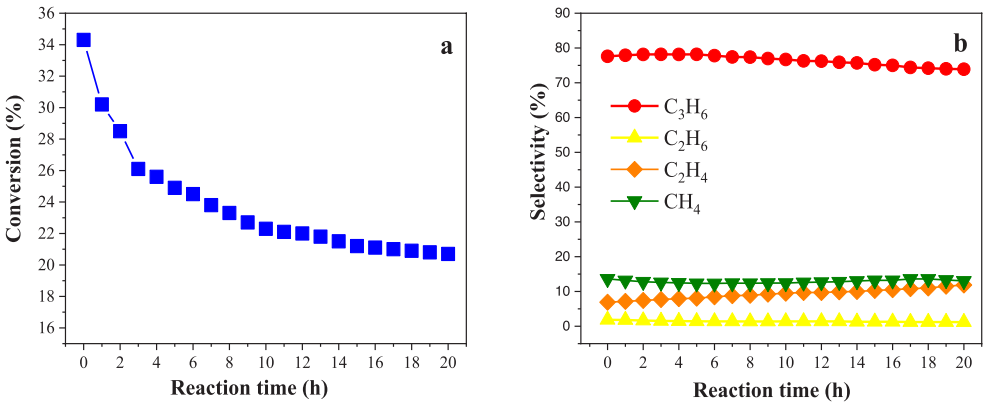

Fig. 11. Propane conversion and selectivity for the reaction products of the 7 Ga/SiO_2-A catalyst over time at a temperature of 650 ℃.

studied catalysts and supports, respectively.

The absorption band at 2114–2120 cm^{-1} is present in the spectra of adsorbed acetonitrile on all samples and is assigned to the bending vibrations of the C-D bonds in the CD_3 group.

Thus, the results of diffuse reflectance IR spectroscopy confirmed an increase in the number of weak acid sites when gallium oxide was deposited on SiO_2.

3.2. Dehydrogenation of propane in the presence of CO_2

The synthesized samples were studied in the reaction of propane dehydrogenation in the presence of CO_2:

$C_3H_8 + CO_2 \rightarrow C_3H_6 + CO + H_2O$

In addition to the formation of propylene, the formation of by-products such as methane, ethane, and ethylene was observed.

The results of catalytic tests at various temperatures are shown in Table S3 and Figs. 9–11. For comparison, Table S3 shows the results of catalytic tests in an empty reactor, in the presence of SiO_2-A, and in the presence of Ga/SiO_2 catalyst systems. It should be noted that in an empty reactor and in the presence of SiO_2-A, the formation of propylene is observed at a temperature of 750 °C, while by-products such as ethane, ethylene, and methane are formed already at low temperatures. It should also be noted that CO is formed as a by-product of the reaction, in the H_2/CO ratio up to 0.1.

The results of the measurements of the catalytic activity at a temperature of 650 ℃ are shown in Fig. 9. The propylene selectivity in the process of propane dehydrogenation increases with increasing gallium content, reaching a saturation. The negligible propylene selectivity at the propane conversion of 4% for the 3 Ga/SiO_2-A catalyst is probably due to the incomplete formation of the active state of gallium species responsible for the main reaction. In this case, side reactions (1–3) may occur, which are thermodynamically more favorable than reaction (4):

$C_3H_8 \rightarrow C_2H_4 + CH_4$, $\Delta H^\circ_{298} = -126{,}4$ kJ/mol (1)

$C_3H_8 + H_2 \rightarrow C_2H_6 + CH_4$, $\Delta H^\circ_{298} = -55{,}67$ kJ/mol (2)

$C_3H_8 + 2H_2 \rightarrow 3CH_4$, $\Delta H^\circ_{298} = -120{,}75$ kJ/mol (3)

$C_3H_8 + CO_2 \rightarrow C_3H_6 + CO + H_2O$; $\Delta H^\circ_{298} = +121$ kJ/mol (4)

With an increase in the gallium oxide content in the samples, a decrease in the catalytic activity is observed, which, according to the results of physicochemical analysis, is most likely due to an increase in the size of metal oxide particles due to the formation of crystalline Ga_2O_3 and blocking of a part of the pores by the supported phase.

For all catalysts, an increase in the propane conversion and propylene selectivity is observed with an increase in the content of the active component in the samples. Accordingly, the highest catalytic activity was found for the samples with a content of 7 wt% gallium for all the studied supports (Supplementary Information, Table S3). Fig. 10 shows

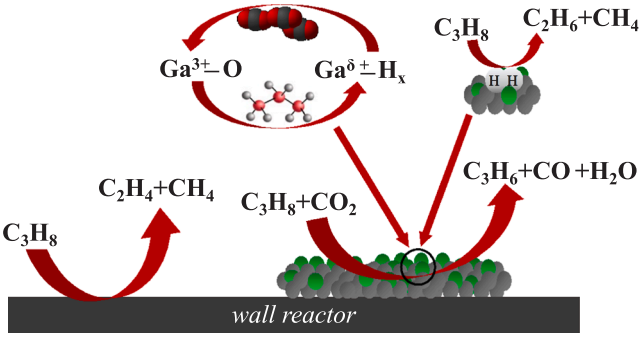

Fig. 12. Scheme of the reaction of propane dehydrogenation in the presence of CO_2.

the temperature dependences of the propane conversion and propylene selectivity for 7 Ga/SiO_2-A, 7 Ga/SiO_2-B, 7 Ga/SiO_2-C catalysts. The catalytic properties of gallium samples differ significantly depending on the textural characteristics of the support. The initial propane conversion of catalysts decreases in the following order:

7 Ga/SiO_2-A > 7 Ga/SiO_2-B > 7 Ga/SiO_2-C.

It should also be noted that the catalytic characteristics perfectly correlate with the data on the catalyst surface acidity, which indicates the importance of the content of surface acid sites in achieving a high catalytic activity of Ga/SiO_2 catalysts.

In this connection, it can be concluded that the catalytic activity of 7 Ga/SiO_2 catalysts correlates with the specific surface area, which is probably due to an increase in the content of acid sites on the support surface and the adsorption capacity of H_2.

As the temperature rises, the propane conversion increases to 68% at T = 750 ℃, and the propylene selectivity decreases to 52%.

The stability of the 7 Ga/SiO_2-A catalyst in the reaction of propane dehydrogenation in the presence of CO_2 at a temperature of 650 ℃ and atmospheric pressure was studied (Fig. 11).

It should be noted that the propylene selectivity was 77% with continuous catalyst operation for more than 20 h, while a decrease in propane conversion from 34% to more than 20% is observed after 10 h of continuous catalyst operation, further, the conversion remains at the level of 20%, from 10 to 20 h remains at the level of 20%.

Thus, according to the results of catalytic tests, reaction schemes 1–4 can be represented as follows (Fig. 12). According to the presented scheme, the reactor wall is the catalyst for the formation of by-products (reaction 1). The main process (reaction 4) that occurs on the catalyst surface can be represented in the form of two stages, the first stage is the dehydrogenation of propane to propylene, as a result of which the particles of gallium oxide interact with hydrogen to form particles of

Table 2
Comparison of the catalytic activity of Ga-containing catalysts in the ODP-CO_2 reaction.

Material	Experimental conditions	T, ℃	Conversion of C_3H_8, %	Selectivity to C_3H_6, %	Productivity, $g(C_3H_6)*kg_{cat}^{-1}*h^{-1}$	Source
7 Ga/SiO_2 (A)	C_3H_8:CO_2	600	21	81	382	This work
$Ga_8Al_2O_{15}$	C_3H_8:CO_2:N_2	500	50	92	65	[13]
5%Ga_2O_3/SiO_2	C_3H_8:CO_2:N_2	600	6.4	92	17	[15]
β-Ga_2O_3	C_3H_8:CO_2:N_2	500	23	94	30	[23]
Ga_2O_3	C_3H_8:CO_2:He	550	44	90	57	[34]

gallium hydride $Ga^{\delta+}H_x$ [33], which in the second stage reacts with CO_2 again forming particles of Ga_2O_3, CO, and H_2O. It should also be noted that hydrogen adsorbed on the catalyst surface can react with propane to form ethane and methane as by-products (reaction 2).

Table 2 shows a comparison of the tested samples with the literature data. In order to compare the catalytic performance of the studied materials with other prospective catalysts, it is reasonable to use such parameter as the productivity since it takes into account experimental conditions. Thus, comparing our results with the literature data, we should note that the obtained catalytic systems demonstrate a much higher efficiency in the ODP-CO_2 reaction. It should also be noted that the 7 Ga/SiO_2-A catalyst exceeds the catalysts studied in the literature in terms of the continuous operation time, more than 20 h.

4. Conclusions

The nature and texture of the support has a significant effect on the catalytic activity of gallium catalysts in dehydrogenation of propane in the presence of CO_2, since supports of the same chemical nature, but with different physical properties, exhibit different BAC strength and adsorption capacity. The strongest BACs are found for the support with a high surface area SiO_2-A and the 7 Ga/SiO_2-A catalyst. It should be noted that the catalytic activity of Ga/SiO_2 catalysts correlates with the specific surface area of the support.

Oxidative dehydrogenation of propane in the presence of CO_2 on gallium catalysts proceeds with a high selectivity and propylene yield. The highest propylene selectivity of 84% and propane conversion of 33% were observed for the 7 Ga/SiO_2-A catalyst, and the lifetime of this catalyst was more than 20 h.

CRediT authorship contribution statement

Marina A. Tedeeva: Methodology. **Alexander L. Kustov:** Data curation. **Petr V. Pribytkov:** Writing – original draft. **Gennady I. Kapustin:** Visualization. **Alexander V. Leonov:** Investigation. **Olga P. Tkachenko:** Conceptualization. **Obid B. Tursunov:** Software. **Nikolay D. Evdokimenko:** Validation. **Leonid M. Kustov:** Supervision, Writing – review & editing.

Declaration of Competing Interest

The authors declare that they have no known competing financial interests or personal relationships that could have appeared to influence the work reported in this paper.

Acknowledgements

The authors thank Dr. V.D. Nissenbaum (Zelinsky Institute of Organic Chemistry) for performing TG-DTG-DTA studies of the samples and Dr. K.B. Kalmykov (Lomonosov Moscow State University) for assistance in SEM studies of the catalyst samples.The work in the part related to catalyst preparation and catalytic tests was carried out with a financial support from Russian Science Foundation, grant no. 20-73-10106. The work in the part of study of catalysts by physicochemical methods was carried out with a financial support by the Ministry of Science and Higher Education of the Russian Federation (project no. 075-15-2021-591).

Appendix A. Supplementary data

Supplementary data to this article can be found online at https://doi.org/10.1016/j.fuel.2021.122698.

References

[1] Balcaen V, Sack I, Olea M, Marin GB. Transient kinetic modeling of the oxidative dehydrogenation of propane over a vanadia-based catalyst in the absence of O_2. Appl Catal A 2009;371(1-2):31–42.
[2] Atanga MA, Rezaei F, Jawad A, Fitch M, Rownaghi AA. Oxidative dehydrogenation of propane to propylene with carbon dioxide. Appl Catal B 2018;220:429–45.
[3] Perez-Ramirez J, Gallardo-Llamas A. N_2O-mediated propane oxidative dehydrogenation over steam-activated iron zeolites. J Catal 2004;223:382–8.
[4] Wu G, Hei F, Zhang N, Guan N, Li L, Grünert W. Oxidative dehydrogenation of propane with nitrous oxide over Fe-ZSM-5 prepared by grafting: Characterization and performance. Appl Catal A 2013;468:230–9.
[5] Dury F, Centeno MA, Gaigneaux EM, Ruiz P. An attempt to explain the role of CO_2 and N_2O as gas dopes in the feed in the oxidative dehydrogenation of propane. Catal Today 2003;81(2):95–105.
[6] Orlyk SM, Kantserova MR, Chedryk VI, Kyriienko PI, Balakin DY, Millot Y, et al. Ga (Nb, Ta)SiBEA zeolites prepared by two-step post-synthesis method: acid–base characteristics and catalytic performance in the dehydrogenation of propane to propylene with C_O2. J Porous Mater 2021;28(5):1511–22.
[7] Mishanin II, Bogdan VI. Advantages of ethane oxidative dehydrogenation on the $MoVNbTeO_x$ catalyst under elevated pressure. Mendeleev Commun 2019;29:455–7.
[8] Djinović P, Zavašnik J, Teržan J, Jerman I. Role of CO_2 during oxidative dehydrogenation of propane over bulk and activated-carbon supported cerium and vanadium based catalysts. Catal Lett 2021;151(10):2816–32.
[9] Tedeeva MA, Kustov AL, Pribytkov PV, Kustov LM. Dehydrogenation of propane in the presence of CO_2 on a 3% Cr/SiO_2 catalyst under supercritical conditions. Mendeleev Commun 2019;30:195–7.
[10] Ramesh Y, Thirumala Bai P, Hari Babu B, Lingaiah N, Rama Rao KS, Prasad PSS. Oxidative dehydrogenation of ethane to ethylene on Cr_2O_3/Al_2O_3–ZrO_2 catalysts: the influence of oxidizing agent on ethylene selectivity. Appl Petrochem Res 2014;4:247–52.
[11] Grabowski R. Kinetics of oxidative dehydrogenation of C_2–C_3 alkanes on oxide catalysts. Catal Rev 2006;48(2):199–268.
[12] Ansari MB, Park S-E. Carbon dioxide utilization as a soft oxidant and promoter in catalysis. Energy Env Sci 2012;5(11):9419. https://doi.org/10.1039/c2ee22409g.
[13] Chen M, Xu J, Su F, Liu Y, Cao Y, He H, et al. Dehydrogenation of propane over spinel-type gallia–alumina solid solution catalysts. J Catal 2008;256(2):293–300.
[14] Sattler JJHB, Gonzalez-Jimenez ID, Luo L, Stears BA, Malek A, Barton DG, et al. Platinum-promoted Ga/Al_2O_3 as highly active, selective, and stable catalyst for the dehydrogenation of propane. Angew Chem Int Ed Engl 2014;53(35):9251–6.
[15] Xu B, Zheng B, Hua W, Yue Y, Gao Z. Support effect in dehydrogenation of propane in the presence of CO_2 over supported gallium oxide catalysts. J Catal 2006;239(2):470–7.
[16] Lei T-q, Cheng Y-h, Miao C-x, Hua W-M, Yue Y-H, Gao Zi. Silica-doped TiO_2 as support of gallium oxide for dehydrogenation of ethane with CO_2. Fuel Proc Technol 2018;177:246–54.
[17] Agafonov YA, Gaidai NA, Lapidus AL. Propane dehydrogenation on chromium oxide and gallium oxide catalysts in the presence of CO_2. Kinet Catal 2018;59(6):744–53.
[18] Tedeeva MA, Kustov AL, Pribytkov PV, Leonov AV, Dunaev SF. Dehydrogenation of propane with CO_2 on supported CrO_x/SiO_2 catalysts. Russ J Phys Chem A 2018;92:2403.
[19] Davydov AA. Molecular spectroscopy of oxide catalyst surfaces. Wiley Interscience Publ. 2003;466.
[20] Hadjiivanov KI, Vayssilov GN. Characterization of oxide surfaces and zeolites by carbon monoxide as an IR probe molecule. Adv Catal 2002;47:307–511.
[21] Berbenni V, Milanese C, Bruni G, Marini A. Thermal decomposition of gallium nitrate hydrate $Ga(NO_3)_3\times xH_2O$. J Therm Anal Calorim 2005;82(2):401–7.
[22] Zheng B, Hua W, Yue Y, Gao Z. Dehydrogenation of propane to propene over different polymorphs of gallium oxide. J Catal 2005;232(1):143–51.
[23] Dooley KM, Chang C, Price GL. Effects of pretreatments on state of gallium and aromatization activity of gallium/ZSM-5 catalysts. Appl Catal A 1992;84(1):17–30.

[24] Burova MV, Fionov AV, Tveritinova EA, Kharlanov AN, Lunin VV. The electron acceptor and catalytic properties of zirconium dioxide modified with aluminum and gallium oxides. J Phys Chem A 2007;81(2):164–9.
[25] Kwak BS, Sachtler WMH. Characterization and testing of Ga/HZSM-5 prepared by sublimation of $GaCl_3$ into HZSM-5. J Catal 1993;141:729–32.
[26] Kazansky VB, Serykh AI. Unusual localization of zinc cations in MFI zeolites modified by different ways of preparation. Phys Chem Chem Phys 2004;6(13): 3760. https://doi.org/10.1039/b401853b.
[27] Mehdad A, Gould NS, Xu B, Lobo RF. Effect of steam and CO_2 on ethane activation over Zn-ZSM-5. Catal Sci Technol 2018;8(1):358–66.
[28] Michorczyk P, Ogonowski J. Dehydrogenation of propane to propene over gallium oxide in the presence of CO_2. Appl Catal A: General 2003;251:425–33.
[29] Lin L, Zhang X, He N, Liu J, Xin Q, Guo H. Operando dual beam FTIR study of hydroxyl groups and Zn species over defective HZSM-5 zeolite supported zinc catalysts. Catalysts 2019;9(1):100. https://doi.org/10.3390/catal9010100.
[30] Medin AS, Borovkov VY, Kazansky VB, Pelmentschikov AG, Zhidomirov GM. On the unusual mechanism of Lewis acidity manifestation in HZSM-5 zeolites. Zeolites 1990;10(7):668–73.
[31] Haney MA, Franklin JL. Mass-spectrometric determination of the proton affinities of various molecules. J Phys Chem 1969;73(12):4328–31.
[32] Angell CL, Howell MV. Infrared spectroscopic investigation of zeolites and adsorbed molecules. IV. Acetonitrile. J Phys Chem 1969;73:2551.
[33] Purcell KF, Grado RS. Studies of the bonding in acetonitrile adducts. J Am Chem Soc 1966;88:919.
[34] Liu Yi, Zhang G, Wang J, Zhu J, Zhang X, Miller JT, et al. Promoting propane dehydrogenation with CO2 over Ga_2O_3/SiO_2 by eliminating Ga-hydrides. Chin J Catal 2021;42(12):2225–33.